GeoHealth

RESEARCH ARTICLE
10.1029/2021GH000575

Special Section:
Community Engaged Research to Action: Examples from GeoHealth

Resolving and Predicting Neighborhood Vulnerability to Urban Heat and Air Pollution: Insights From a Pilot Project of Community Science

Jun Wang[1,2], Lorena Castro-Garcia[1], G. Darrel Jenerette[3], Mark Chandler[4], Cui Ge[1], Dion Kucera[3], Sofia Koutzoukis[3], and Jing Zeng[1,2]

[1]Center for Global & Regional Environmental Research and Iowa Technology Institute, The University of Iowa, Iowa City, IA, USA, [2]Department of Chemical and Biochemical Engineering, Department of Physics and Astronomy, The University of Iowa, Iowa City, IA, USA, [3]Department of Botany and Plant Sciences, University of California, Riverside, CA, USA, [4]Earthwatch Institute, Boston, MA, USA

Abstract Urban heat and air pollution, two environmental threats to urban residents, are studied via a community science project in Los Angeles, CA, USA. The data collected, for the first time, by community members, reveal the significance of both the large spatiotemporal variations of and the covariations between 2 m air temperature (2mT) and ozone (O_3) concentration within the (4 km) neighborhood scale. This neighborhood variation was not exhibited in either daily satellite observations or operational model predictions, which makes the assessment of community health risks a challenge. Overall, the 2mT is much better predicted than O_3 by the weather and research forecast model with atmospheric chemistry (WRF-Chem). For O_3, diurnal variation is better predicted by WRF-Chem than spatial variation (i.e., underestimated by 50%). However, both WRF-chem and the surface observation show the overall consistency in describing statistically significant covariations between O_3 and 2mT. In contrast, satellite-based land surface temperature at 1 km resolution is insufficient to capture air temperature variations at the neighborhood scale. Community engagement is augmented with interactive maps and apps that show the predictions in near real time and reveals the potential of green canopy to reduce air temperature and ozone; but different tree types and sizes may lead to different impacts on air temperature, which is not resolved by the WRF-Chem. These findings highlight the need for community science engagement to reveal otherwise impossible insights for models, observations, and real-time dissemination to understand, predict, and ultimately mitigate, urban neighborhood vulnerability to heat and air pollution.

Plain Language Summary Heat waves and air pollution events can often occur at the same time, posing a dual threat to the public health in many urban neighborhoods. However, at or within the neighborhood scale (a couple of kilometers or less), few measurements have been taken via community engagement and little is known quantitatively about the covariation of ozone and temperature. Here, we present a summer pilot project of community science that involved ~1,000 (including ~750 K-12 students) people to study urban heat and ozone pollution in various neighborhoods in Los Angeles, CA. We summarize the methods and findings of the community engagement. Precious data collected by the community members reveals large spatial variations of ozone and temperature at the neighborhood scale, which are not resolved in the current generation of the operational (hourly) air quality forecast predictions or satellite data products. However, with observations suggesting the significant impact of canopy on air temperature and model's reliable performance in predicting observed strong ozone-temperature covariations, we suggest that green space has the potential to simultaneously mitigate the community's vulnerability to high temperature and air pollution. Future work is needed, especially via community engagement in other urban areas, to study ozone, temperature, and vegetation nexus.

Key Points:

- A summer project of community science involving ~1,000 participants is presented to study urban heat and ozone pollution in Los Angeles, California
- Neighborhood variation of and covariations between air temperature and ozone amount are significant and poses challenges for models
- Community engagement reveals otherwise impossible insights for research and real-time dissemination on heat and air pollution vulnerability

Supporting Information:

Supporting Information may be found in the online version of this article.

Correspondence to:

J. Wang,
jun-wang-1@uiowa.edu

Citation:

Wang, J., Castro-Garcia, L., Jenerette, G. D., Chandler, M., Ge, C., Kucera, D., et al. (2022). Resolving and predicting neighborhood vulnerability to urban heat and air pollution: Insights from a pilot project of community science. *GeoHealth*, *6*, e2021GH000575. https://doi.org/10.1029/2021GH000575

Received 10 DEC 2021
Accepted 13 MAR 2022

Author Contributions:

Conceptualization: Jun Wang, G. Darrel Jenerette, Mark Chandler, Jing Zeng
Data curation: Jun Wang, Lorena Castro-Garcia, G. Darrel Jenerette, Mark

1. Introduction

Many urban regions are facing dual threats as a result of increasing air pollutants and temperatures (IPCC, 2021). With global demographic trends projecting 2.5 billion more urban residents by 2,050, the negative impacts of high urban heat and air pollution are expected to rise (Hong et al., 2019; Jacob & Winner, 2009; Nolte et al., 2018). Retrofitting current cities and designing future ones to reduce health impacts associated with hotter and more

Chandler, Cui Ge, Dion Kucera, Sofia Koutzoukis
Formal analysis: Jun Wang, Lorena Castro-Garcia, Mark Chandler, Jing Zeng
Funding acquisition: Jun Wang, G. Darrel Jenerette, Mark Chandler
Investigation: Jun Wang, Lorena Castro-Garcia, G. Darrel Jenerette, Mark Chandler, Cui Ge, Dion Kucera, Sofia Koutzoukis, Jing Zeng
Methodology: Jun Wang, G. Darrel Jenerette, Mark Chandler, Jing Zeng
Project Administration: Jun Wang, G. Darrel Jenerette, Mark Chandler
Resources: Jun Wang, G. Darrel Jenerette
Software: Jun Wang, Lorena Castro-Garcia, Cui Ge, Jing Zeng
Supervision: Jun Wang, Mark Chandler
Validation: Jun Wang, Lorena Castro-Garcia
Visualization: Jun Wang, Lorena Castro-Garcia, G. Darrel Jenerette, Mark Chandler, Cui Ge
Writing – original draft: Jun Wang, Mark Chandler
Writing – review & editing: Jun Wang, G. Darrel Jenerette, Mark Chandler

polluted urban environments is a critical need, and increasing urban vegetation has become an important policy goal of many urban policy makers. Some modeling studies are suggestive of reductions in heat and air quality risks (Escobedo & Nowak, 2009; Morani et al., 2011) associated with O_3 removal by urban trees in the U.S. (Nowak et al., 2014). Others, however, argued that tree types also matter and affect amount and type of biogenetic volatile organic compounds (VOCs), leading to different ozone formation potential (Gu et al., 2021). In cities such as Los Angeles, co-occurrences of heat waves and high O_3 concentration are common, likely due to the increase of VOCs from trees and more stagnant air, both associated with high temperature days (Nussbaumer & Cohen, 2020). While the anticorrelation between vegetation fraction and temperature as well as the positive correlation between temperature and O_3 are both well established in the literature (Nussbaumer & Cohen, 2020; Pusede et al., 2015), the data underpinning model-based assessment at the urban scale are severely limited (Tong et al., 2015), and comparisons with few field observations have less clear implications (Churkina et al., 2015; Pataki et al., 2011). Notably, in the urban environment, especially at the neighborhood scale on the order of kilometers or less, the variation of human-environment interaction is seldom studied simultaneously for O_3 and temperature due to the dearth of observation data (Cabaraban et al., 2013; Shiflett et al., 2017) except in some cases using mobile facility for a time duration of a week or less (Samad & Vogt, 2020); however, these are the scales appropriate for interventions and policies that can reduce environmental risks (Harlan et al., 2013).

Resolving an individual's interactions with the environment is critical for understanding the environmental conditions underpinning the neighborhood vulnerability and thereby improving decision making by both individuals and policy makers. High-resolution satellite data such as that from Landsat has pixel size of 30–90 m (Tomlinson et al., 2011), they, however, lack temporal coverage, especially in cloudy conditions. On a daily basis, existing satellite-based products are at ~0.5–1 km resolution at best for land surface temperature (LST) and phenology characteristics, for example, from the Moderate Resolution Imaging Spectroradiometer (MODIS) (Wan et al., 2004), and at the city scale for indicators of air quality at 7–10 km resolution, for example, atmospheric loading of NO_2 from the TROPOspheric Monitoring Instrument (TROPOMI) (Griffin et al., 2019). Furthermore, neither satellite-based LST nor air pollution data represents the air temperature and surface pollution concentration, often measured at 2 m above the surface. At the same time, spatial distribution of ground-based monitoring networks is at such a low density that it is not possible to resolve neighborhood variations. For example, within the greater Los Angeles megapolitan region there are only ~25 O_3 reporting stations, with spatial layout incapable to characterize the joint occurrence of high O_3 and temperatures at intra-neighborhood scale or within 4–5 km—The typical spatial resolution (~4 km) of a regional air quality model.

Here, we present a pilot study using a community science project to address urban heat and air pollution challenges at the neighborhood and intra-neighborhood scales, including taking measurements to evaluate the fidelity and deficiency of the satellite and regional model (Weather Research and Forecast coupled with Chemistry, or WRF-Chem, configured with common practice for operational air quality forecast) at these scales. At intra-neighborhood scale, O_3 can be hypothesized to have large variations because of the short (from hours to less than a day) lifetimes (especially in the summer) and heterogeneity of emission sources in space and time for NOx and VOC (Racherla & Adams, 2008), as well as the spatiotemporal variation of solar radiation and temperature at the surface caused by trees and building shadows. Understanding the processes associated with this hypothesis requires the data from spatially dense observations that, without community engagement, can be challenging to obtain. Pusede et al. (2015) reviewed the dependence of O_3 formation process on air temperature, while Shiflett et al. (2017) showed large spatial variations of air temperature at the intra-neighborhood scale. To date, collocated measurements of O_3 and air temperature in the neighborhood and intra-neighborhood scales are still rare.

Originally designed as a citizen science project, our community science project engages with all residents, both citizens and noncitizens. According to the National Academies of Sciences and Medicine (2018), "citizen science projects are those that typically involve nonscientists (i.e., people who are not professionally trained in project-relevant disciplines) in the processes, methods, and standards of research, with the intended goal of advancing scientific knowledge or application." For example, citizen science projects have been used to evaluate the radar-estimated precipitation and hurricane intensity characterization (Elmore et al., 2014). In the context of satellite remote sensing, the Students' Cloud Observations On-Line (S'COOL) project and the Global Learning and Observations to Benefit the Environment (GLOBE) program are examples that show the value of citizen science data for assessing satellite-based products of cloud fraction, for example, (Chambers et al., 2017; Kennedy & Henderson, 2003). A recent literature survey found that the data from citizen science observations

can reveal insights into people's perceptions and exposure levels at the neighborhood scale (Mahajan et al., 2020). However, a community science project focusing on both urban heat and air pollution has not been reported in the literature, let alone one that integrates community engagement and community science with the model predictions, satellite data analysis, and real time delivery of results.

2. Community Science Sensor Network and Campaigns

We designed our study to assess temperature and O_3 variation at multiple scales, from individual parcels to the Los Angeles metropolitan region (Figure 1a) in summer 2017. We organized sensor deployments around individual neighborhoods, which we defined as 4×4 km^2 quadrats. The intensive field deployment has focused on various parts of Long Beach and the Inland Empire in California (Figures 1c–1h), a subset of the Los Angeles megapolitan region with severe nonattainment of O_3. The deployment duration was divided into three campaigns. In the first campaign of June–July 2017, six sensor nodes were distributed into two quadrats (three sensor nodes per quadrat) within a distance of less than 20 km (e.g., quadrats 1A and 1B in Figure 1) in the neighborhoods of Long Beach. With this design, the quadrat size is comparable to the nominal spatial resolution of air quality models and EPA emission inventories, which are often at 4×4 km^2, while the distance between the two quadrats is comparable to the dimension of the TROPOMI footprint (4×7 km^2) at the nadir. Consequently, the distribution of the community science network is well suited to taking measurements to address questions concerning model uncertainties at the sub-grid scale and satellite retrieval uncertainties at the sub-pixel resolution. The deployments in the second campaign of July–August and the third campaign of August–September 2017 were similar to that of the first phase, but for different quadrats in the neighborhoods of Claremont (2A and 2B in Figure 1) and San Bernardino (3A and 3B), respectively. While the two quadrats are paired at each phase of the project to measure the sub-regional gradient expected temperature and O_3, the neighborhood pairs in all three phrases of the project were selected to collectively reflect a regional gradient.

In each of the quadrats, three custom-built sensor nodes (Figure 1b) were laid out to sample as much air from different environmental settings (such as parking lots, residential backyards, and tree-shaded areas) as possible. The iButton network consisted of ∼290 sensors that were placed within each neighborhood through a community science partner design but still covered a comprehensive distribution of conditions through each neighborhood. The iButton sensors were placed above baer soil and irrigated grass and underneath tree canopies, and only data collected 2 m above the surface is used for this study. The locations of these 2 m sensors are shown as yellow dots in Figures 1c–1h for a total of six quadrats. Each iButton was shielded with a custom-made white vented cap and was programmed to record data hourly. The iButton temperature readings were calibrated and found to have an accuracy of ±1.0°C; they were archived together with the time when each measurement was taken. Details on using iButton-measured temperatures for studying urban air temperature are provided by Shiflett et al. (2017).

Each sensor node integrates micrometeorological and O_3 sensors (Figure 1a) that enable spatial and temporal coincident measurements of O_3, wind, and temperature, simultaneously, at each hour. Unique to the sensor node is a high-end O_3 analyzer, 106-L (2B Technologies, Boulder, CO) to measure O_3 concentration at 2 m. The 106-L instrument was designated by the EPA as a Federal Equivalent Method (FEM) for monitoring in compliance with the US Clean Air Act (EQOA–0914–218). Also integrated on the node are weather sensors, including anemometers for measuring wind direction and speed, and thermometers (HMP-60 in a standard radiation shielding (41003-5, Campbell Scientific, Logat UT) to measure temperature, all placed 2 m above the surface. Each sensor node was connected to the internet, using either household Wi-Fi or a cellphone hotspot, enabling real-time data transfer to the data server.

For both the sensor nodes and the iButtons, we conducted periodically a series of calibration and validation studies in both a controlled atmospheric chamber and field conditions; the uncertainty of measured O_3 is about 1–2 ppb and the uncertainty of temperature data is ±1.0°C. All sensor data, both from the sensor nodes and the iButton temperature, were measured hourly. All sensor deployment and data collected by the community were overseen by a project staff. Data were reviewed and problematic data were reassessed by the project team for inclusion in analyses.

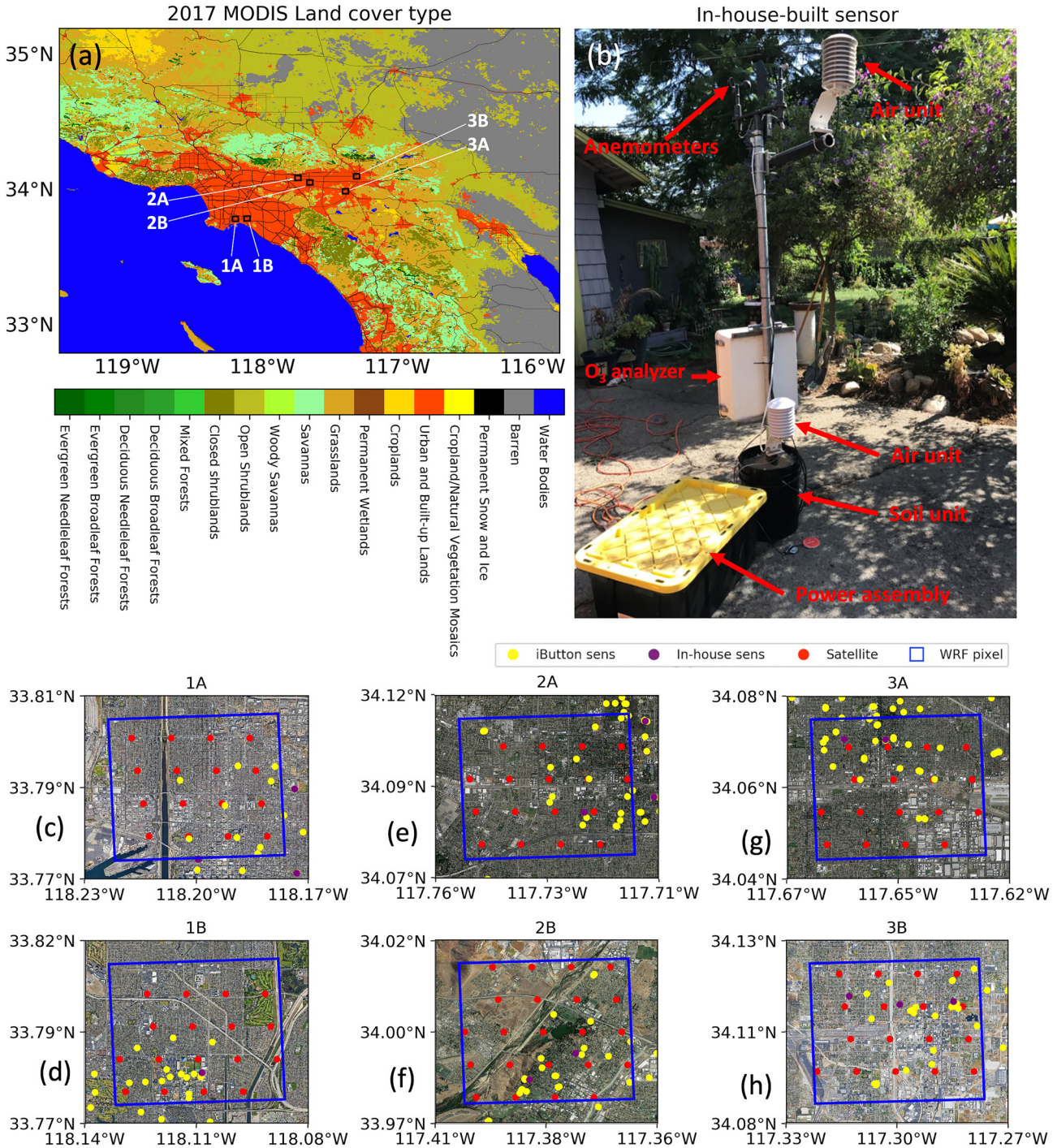

Figure 1. (a) Moderate Resolution Imaging Spectroradiometer (MODIS) land surface cover type. (b) A picture of an in-house-built air-O_3 sensor node showing the assembly of multiple sensors to measure wind (by anemometers), temperature, relative humidity and pressure (by sensors in air unit), O_3 concentration (by O_3 analyzer) in the air, all at 2 m above the surface, as well as soil moisture (by soil unit). (c–g) Show the satellite view of each quadrat. The blue rectangle shows the 4×4 km^2 WRF-Chem model grid box that collocates with each quadrat. Also denoted in (b)–(g) are the locations of iButton sensors (in yellow dots), the air-O_3 sensor node (purple), and the MODIS 1×1 km^2 land surface temperature pixels (red) within corresponding weather and research forecast-Chem grid box (blue square).

3. Community Science Engagement Activities

We sought to engage a wide range of participants across the study region using more of a collaborative or cocreated model of community science engagement (Shirk et al., 2012). Outreach and recruitment of participants

Figure 2. (a) A flowchart illustration and examples of citizen science engagement. Please see the text for details. (b) A series of iPhone screenshots showing the Earth System Modeling Complex app that provides citizen access to a wide range of information including the forecast for the next 3 days (first panel on the left), a map of predicted weather (second), an interactive map (third), and a detailed forecast.

(Figure 2a) was done via multiple methods, including contacting participants in existing projects, posting on social media, and leveraging networks of partner organizations (e.g., Aquarium of the Pacific, Chino Basin Water Conservation District, Riverside Corona Resource Conservation District). We hired a Spanish-speaking intern and worked through key community organizers to reach Hispanic populations throughout our region.

Community scientists (e.g., residents interested in science) participated in our project in multiple ways with a goal of creating a cycle from engagement, training, deployment, data collection, and evaluation back to engagement and action. Community workshops (Figure 2) were held for each of the deployment campaigns to provide background; discuss objectives and the collections, use, and access of the data (all publicly open); answer questions; and engage in a community mapping exercise in which community members identified hot (or cool) spots or areas where they thought ozone or temperature was unusual, problematic, or of concern. This feedback helped identify locations for the community-deployed sensor nodes. This high-level engagement provided novel opportunities for community residents to learn about their environment in the context of satellite observations and contributed to valuable measurements in locations we had not planned. Throughout the project, we provided community scientists with opportunities to share information about their experiences with local climate and air quality, to formulate questions and concerns that the project could address, and to shape the research design.

A key community science activity was hosting our sensor nodes in locations where the instruments, local power, and internet connectivity were secure. Community scientists also participated to map the canopy types of local land cover surrounding sensors by using the online Habitat Network tool (https://content.yardmap.org/learn/

habitat-network-intro/) and collecting data about individual trees (such as diameter at breast height and canopy width) in their sampling plot. Training materials were developed collaboratively with local partners. Environmental education specialists within key partner organizations provided input and assistance in setting up in-person training. Participants communicated throughout the sampling period using texting and emails. Following the individual campaigns in each project phase, we engaged participants through a follow-up workshop, blog posts, and individualized reports with results provided both digitally and in mailed hard copies.

Hands-on activities were used to maintain engagement of community residents. For example, they used high-resolution images from Google Maps to classify the different types of landscapes, or habitats, in their neighborhoods with a program called "Habitat Map." Using the program, they drew polygons over a Google Maps image of the property and labeled each polygon (e.g., tree, building, road, and grass). Because the community scientists were familiar with the area and often the property itself, they could identify features at a finer resolution than typical landscape image classification programs. We could then associate each landscape feature with the local sensor (e.g., ozone or air temperature). The data quality is periodically verified via in-person site visit.

In addition to workshops and regular exchanges via texts and email, a key method for science engagement was the on-demand interactive web services and phone apps. The Earth System Modeling Complex (ESMC) web services (https://esmc.uiowa.edu/ca/) and phone app were designed and built to allow participants to visualize the measurements and the forecast as a function of time. The real-time forecast was made using the WRF-Chem (Fast et al., 2006; Grell et al., 2005), which provides prediction of meteorology and air quality for the study domain at 4 km resolution, four times per day, each time for the following 72-hr predictions (see details in the supplement). Descriptions of WRF-Chem real-time runs and the ESMC software infrastructure can be found in the supplement. WRF-Chem is a community model that offers multiple schemes for configuration to predict air quality and weather. The WRF-Chem configuration we have here followed our past studies (Ge et al., 2014, 2017; Wang et al., 2013, 2022; Zhang et al., 2020), although the WRF-Chem model performance can depend on the configuration of various emissions, the parametrization schemes for atmospheric chemistry and dynamics processes (Ge et al., 2017) and the model boundary and initial conditions (Sha et al., 2021). Since the model is used operationally for the purpose of the community engagement, detailed process study is out of the scope for this pilot study. Instead, we studied the fidelity and deficiency of a business-as-usual configuration (without any tuning) for WRF-Chem to be used for the forecast of community air quality and temperature forecast.

The functionality of the phone app (Figure 2b) is similar to that of ESMC but provides residents a user-friendly modular interface at their fingertips to query the information. It also allows users to input their own observations (such as clouds and precipitation amounts) if the forecast is incorrect. The ESMC website content has six parts (as described in the supplement and partially illustrated in Figures S1–S5 in Supporting Information S1). The website provides access to the animation of the forecasted spatial distribution of weather parameters air pollution concentration of O_3 at each four for the next 72 hr. It also enables the community to access forecast data, their observation data, and satellite data via the on-demand interactive map with zoom-in and zoom-out capabilities in their neighborhood of interest, all in real time. This enables them to appreciate the value of the observation data for evaluating real-time predictions.

4. Results

4.1. Community Science Engagement

Across the three deployment campaigns, the project engaged participants from 104 homes, 14 educational institutions (high schools and colleges/universities), and 18 other partner institutions (Figure 2a). We estimate that 238 people were directly engaged in helping to collect field data and/or place the temperature sensors and that an additional ~750 students from K12 schools were also engaged in the deployment of sensors. An additional 100 people were engaged in community workshops (Figure 2a) about air quality or mapping of habitats around sensor sites.

We used two participant feedback mechanisms, one at sensor pick-up and the other an online SurveyMonkey survey sent 1–4 months post sensor deployment. Both found very high rates of satisfaction across our participants. Eighty-six percent of respondents were satisfied or very satisfied with the program, with 5% being unsatisfied. Eighty-nine percent of participants were very interested in the project's results, with the remainder somewhat interested; no respondents were uninterested in project results.

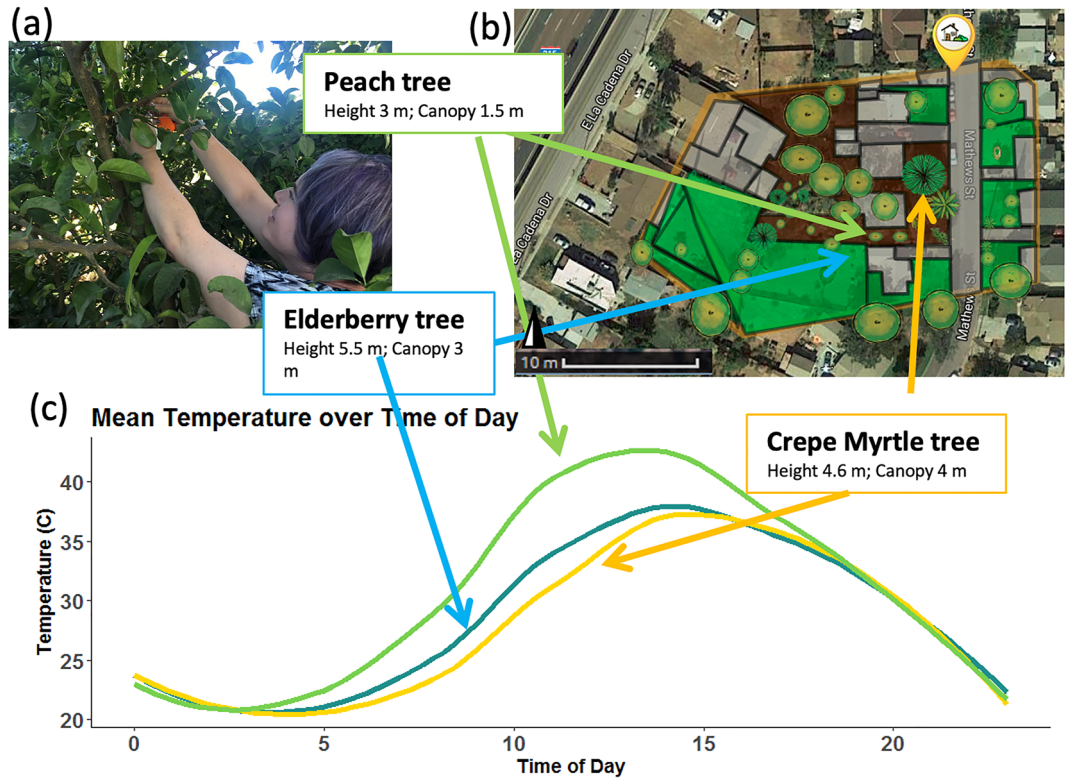

Figure 3. An example showing the impacts of different type of trees on diurnal variation of temperature.

One key finding is that the participants are very enthusiastic on hands-on activities and scientific research that are closely relevant to their neighborhoods. Survey showed that participants are more willing to spend time and accommodate needs for the sensor placement and deployment once we introduce the topic that high temperature and high O_3 can covary and introduce the EMSC dashboard and phone app. Results from the ESMC website dashboard and phone app were presented to all participants in reports and blogs, which helped community members better understand local variation in air quality and air temperature. The dynamic nature of the program, which allowed participants to ask and answer their own questions by choosing different sensors to compare, was of particular interest and encouraged them to ask and answer questions about air quality and temperature in their neighborhoods.

The participants also found the measurements in the neighborhood are revealing and appreciated much more about the importance of canopy to cope with high temperature and O_3. While participants know that green canopy can lower the temperature, they knew little about how the canopy may help to mitigate the O_3 before the community engagement. At least in the neighborhood we studied, O_3 in general decreases with the decrease of air temperature (Section 4.4), which is consistent with the literature (Pusede et al., 2015). These findings from both observations and models are conveyed to the participants via the community engagement, which helped the community as a whole to appreciate more on the role of green canopy for mitigation heat and air pollution at the same time.

An example showing the impacts of different type of trees on diurnal variation of temperature is presented in Figure 3. In the yard of a participant (Figure 3a), iButton air temperature sensors were placed in three different trees (peach, elderberry, and crepe myrtle). The community scientists helped measure the size of each tree. This allowed us to calculate the hourly average air temperature over the 24-hr daily cycle (Figure 3c). The community scientist also mapped the different land covers on their property using the mapping tool (see Figure 3b for results of the mapping effort). It shows clearly that the daytime air temperature under the crepe myrtle tree was lowest likely due to the size of the tree, while the air under the peach tree near the parking lot had the highest temperature. In this case, the temperature could differ by 5°C at around noon (Figure 3c).

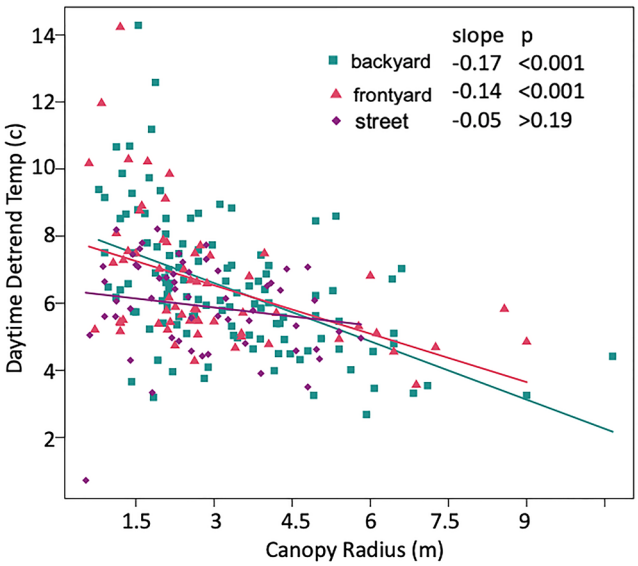

Figure 4. Impacts of canopy radius on daytime detrend temperature. Here, detrend is done by subtracting weekly moving average temperature from the measured temperature at each corresponding location.

Figure 4 shows that the canopy radius has a direct impact on temperature. Here, the canopy radius is the average of distance from the trunk to the branch edge of the tree in four (north, east, west, and south) directions. Larger canopy leads to lower temperature. For an increase of 1 m of canopy radius, the daytime temperature can decrease by 0.15°C and 0.17°C in backyard and front yard settings, respectively, both at the statistically significant level. However, in the street settings, an increase of 1 m of canopy size only leads to a decrease of 0.05°C, and this anticorrelation is insignificant likely reflecting the influence of the heat emitted from and stronger air mixing caused by vehicles on the road.

4.2. Overall Assessment of Satellite Data and Model Predictions

The data collected by the community is used to assess WRF-Chem predictions of O_3 and 2 m air temperature (2mT) at the neighborhood scale. There are many studies that have assessed the performance of WRF in simulating 2mT, but the observation data used is generally disconnected from the community science perspective, that is, using the predictions to engage the community and underline the power of science. The participants are more engaged once they found the model predictions are indeed in many cases comparable with what they measure in their backyard, which in turn brings trustworthiness of the prediction and science to the community to help further engage with the community.

Spatially, Figures 5a and 5c show the mean distribution of O_3 and 2mT predicted for 19:00 UTC (12:00 Pacific Daylight Time, or PDT), the nominal time when the Terra satellite passes. The prediction is initiated 18 hr before

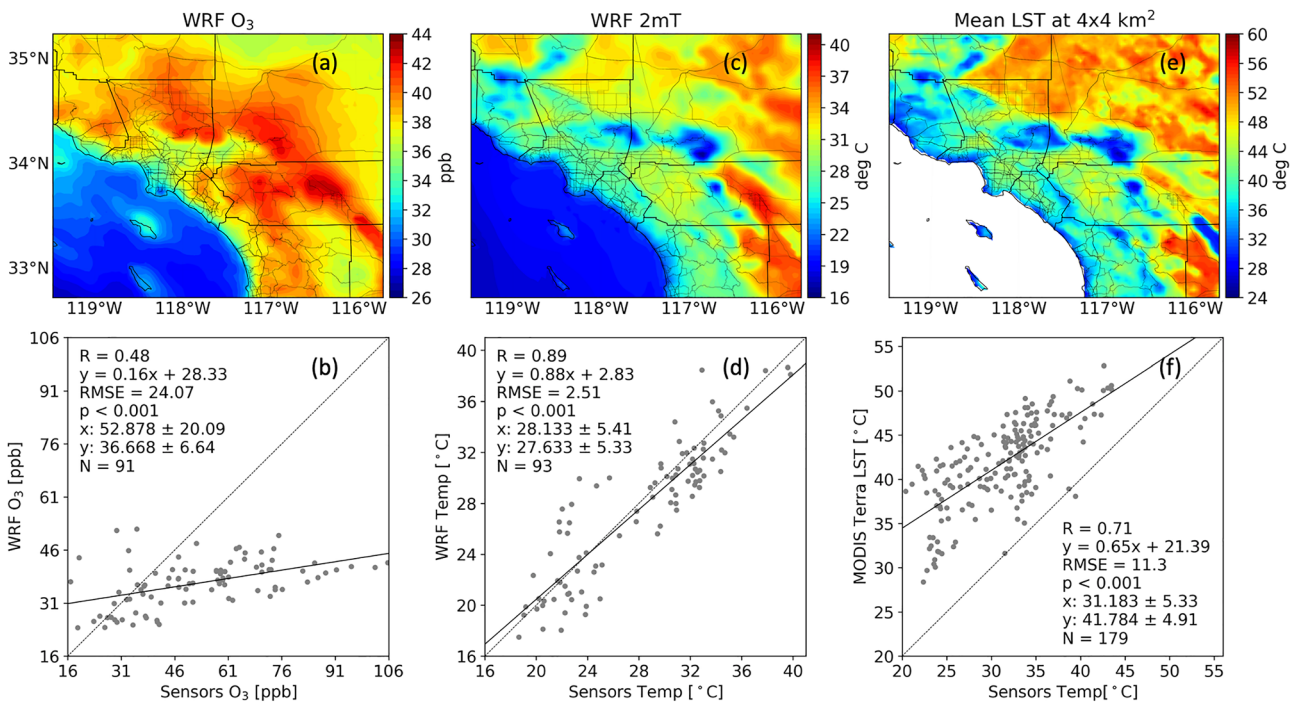

Figure 5. Spatial distribution of weather and research forecast model with atmospheric chemistry forecasts of (a) surface O_3 and (c) air temperature, as well as (e) Moderate Resolution Imaging Spectroradiometer (MODIS) land surface temperature (LST), averaged at 19:00 UTC in July 2017. Also shown are the evaluation of forecast parameters for each day with (b) measured O_3 concentration and (d) measured air temperature. The MODIS LST is also evaluated with 2 m air temperature (2mT) because there is no direction measurement of LST. Statistics of evaluation including the linear correlation coefficient R, the best-fit equation, statistical significance, the mean and standard deviation of the x and y variables, and the number of data points are also shown in each evaluation panel.

the observation. Overall, the WRF-Chem forecasted O_3 correlates with the observed O_3 with a linear correlation coefficient (R) of 0.48 (at a statistically significant level) and a large bias of 16 ppb at the hour of interest. In contrast, correlating with observed 2mT, the predicted 2mT has an R value of 0.85, a mean bias of 0.5°C, and a root-mean-square-error of 2.86°C, while the MODIS LST (with mean spatial distribution shown in Figure 5e) has an R value of 0.71 and a mean overestimation by ∼10°C. This suggests that in urban settings, LST is not necessarily a good indicator of 2mT, as it only explains ∼50% of the variance of 2mT.

While Figure 5 only shows the results valid at 19:00 UTC, our further analysis reveals the following for all other hours (as detailed in the supplement). The predicted temperatures with different lead times all have positive biases, R values from 0.8 to 0.9 with most centered around 0.85, and a normalized standard deviation (with respect to the observation) of ∼80% (Figure S6a in Supporting Information S1). The forecasts in the first 24–30 hr are overall better than those at 48 hr and beyond. In contrast, for O_3 predictions, the normalized standard deviation of prediction is only 40% in the first 6 hours and improves to 50% after 40 hr (Figure S6b in Supporting Information S1). Contrary to the temperature, however, the O_3 predictions for 25–30 hr or later appears to have lower bias, and the predictions made by different hours have similar R values of 0.75. Overall, predicted temperature performs better than predicted O_3 in terms of both R (Figure S7 in Supporting Information S1) and normalized standard deviation. However, model predications for temperature and O_3 both show less than the observed variability, especially for O_3 where model is only able to capture half of the variability (Figure S6a vs. S6b in Supporting Information S1). Apparently, O_3 needs more model spin-up time (up to 12–36 hr), while temperature prediction has the best prediction in the first 30–36 hr with almost no need for spin-up.

We also evaluated our model prediction to answer the question of which time of day the best forecast can be made for the next 72 hr. Overall, no significant differences in forecast performances are found among all four model initialization times, especially for O_3. However, the forecasts initialized at 18:00 UTC appear to match slightly better with observations in terms of the normalized standard deviation for temperature (Figures E6c and S6d in Supporting Information S1). In the section below, unless otherwise stated, we select the third set of predictions (e.g., initialized at 18:00 UTC on the third day ahead of the observation) as an example data set to evaluate the spatial variability of temperature.

4.3. Air Temperature and LST Spatiotemporal Variability

The spatial variability of 2mT (Figure 6a) can be affected by several factors among which the surface properties play a critical role. This is demonstrated clearly in Figure 6b where the spatial variability of 2mT (from WRF-Chem output) is characterized by standard deviation (STD) in 3×3 grid boxes with each box measuring 4×4 km^2. Both the WRF-Chem-simulated spatial distribution (Figure 6a) and spatial variability (Figure 6b) of 2mT resonate with the counterparts of MODIS LST (Figures 6c and 6d), showing good agreement in highlighting larger spatial variability in transition zones, notably from urbanized valleys to mountain tops (e.g., denoted as areas 1, 2, and 3 in Figure 6h), and from the inland water bodies of Salton Sea to their barren surroundings (denoted as area 4 in Figure 6h). Clearly, by combining topography data and MODIS land use data (Figure 1a), one can discern the relatively large inhomogeneities of surface types (barren soil and various types of savannas) in these transition zones. The overall agreement between the spatial variability of MODIS LST and WRF-Chem-simulated 2mT suggests the fidelity of WRF-Chem simulation of land-atmospheric interactions.

At 4 km spatial resolution, the spatial variability of 2mT can be up to 5.6°C in the 12×12 km^2 area surrounded by urban areas, that is, the Palm Spring area (denoted as P in Figure 6b). In contrast, at the same resolution, the LST variation (Figure 6d) can be up to 10°C in the same size area of barren land (area 4 in Figure 6h) surrounding the Salton Sea. The contrast between Figures 6d and 6b suggests that the LST spatial variability is generally larger than the counterpart of 2mT, reflecting the heat dispersion by the atmospheric movement. In the barren lands surrounding the Salton Sea, the LST contrasts enable the formation of land or sea breezes, which can lower the 2mT spatial variability. At daytime, the wind carries lower temperature air from the Salton Sea to the land, and at night, the wind reverses its direction from land to the sea, both of which lead to more atmospheric mixing and therefore more homogenous distribution of O_3 and temperate along the coastal region (Wang et al., 2013). Finally, since the native resolution of MODIS LST is at 1 km, we also compute the STD of LST at resolution of 4×4 km^2 (Figure 6g). The contrast between Figures 6g and 6d clearly shows that the variation of LST is scale dependent. The LST variation at 4×4 km^2 is twice less than that at 12×12 km^2, underscoring the nature of LST variation at the neighborhood scale.

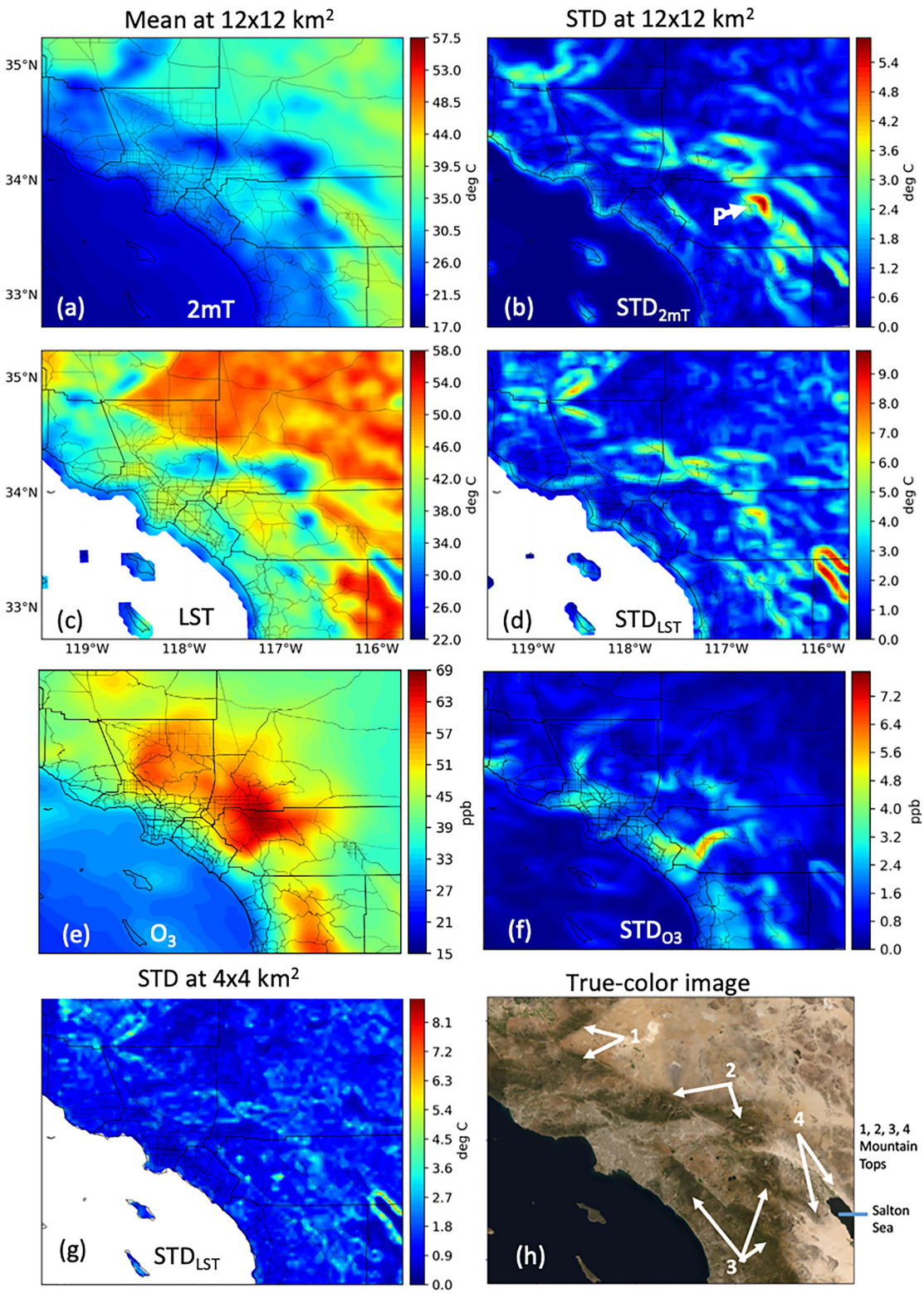

Figure 6. Spatial distribution of (a) weather and research forecast model with atmospheric chemistry (WRF-Chem) forecast of 2mT and (b) its standard deviation (STD), averaged at 19:00 UTC in July 2017 at the spatial resolution of 12×12 km^2 (e.g., 3×3 WRF-Chem 4×4 km^2 grid boxes in the inner most domain). Panels (c and d) are similar to panels (a and b), respectively, but for MODIS LST; (e) and (f) are for WRF-Chem forecasts of O_3. Also shown are (g): the Moderate Resolution Imaging Spectroradiometer land surface temperature (MODIS LST) standard deviation computed at 4×4 km^2 by using MODIS LST at 1×1 km^2 resolution, and (h) a true-color image of the study region with different location marked (see details in the text).

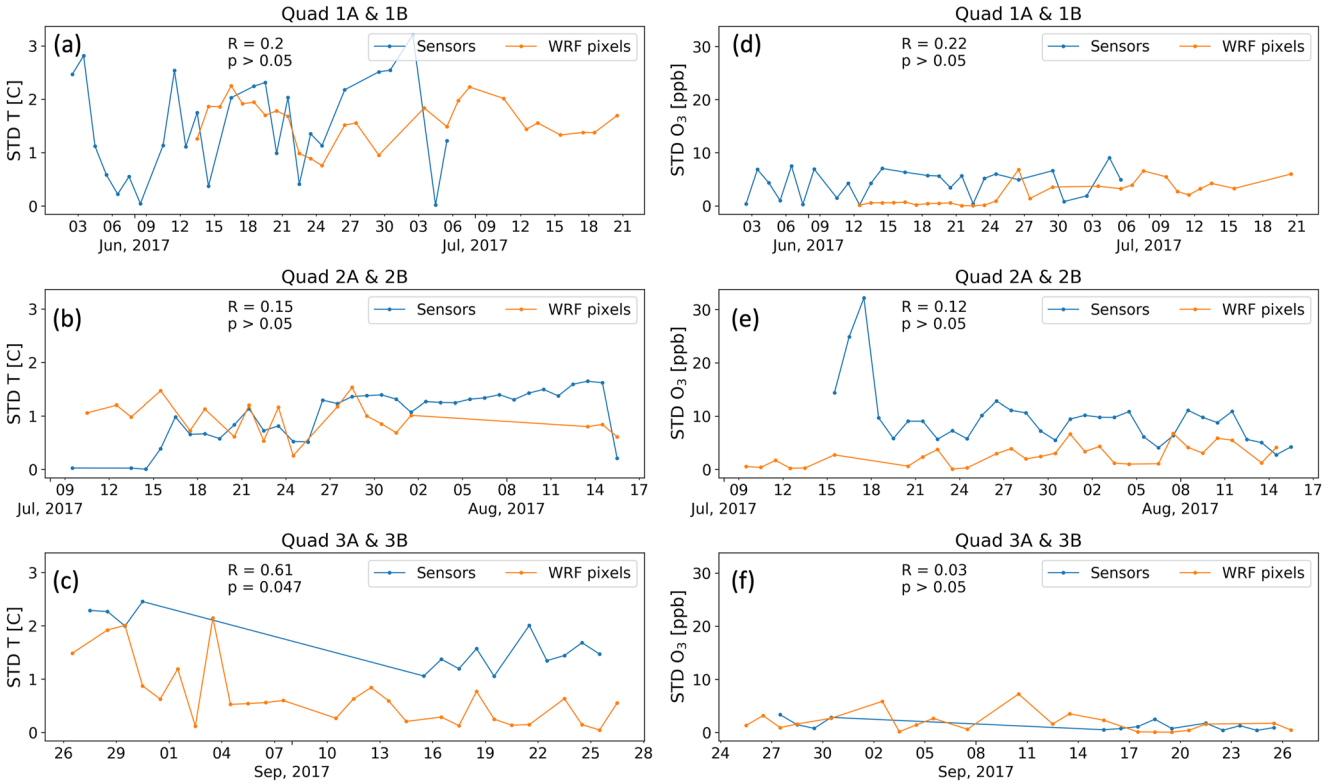

Figure 7. Time series of the standard deviation of daily O_3 (left) and 2mT (right) measured by sensors in each quadrat pair and simulated by weather and research forecast model with atmospheric chemistry (at 4×4 km^2 each). See text for details.

We further compare the LST spatial variability at 4×4 km^2 with the spatial variability of 2mT characterized by all the community science measurements in each quadrat (Figure S8a in Supporting Information S1). The LST variability characterized using MODIS 1 km data showed nearly zero correlation with that of 2mT characterized using all sensors (varying from 22 to 26) in each quadrat at each day of 19:00 UTC. In temporal averages for each quadrat, the correlation of spatial variability between LST and 2mT is poor, with a negative correlation coefficient of −0.44 (Figure S8b in Supporting Information S1). Overall, Figure S8 in Supporting Information S1 and Figure 6 suggest that (a) 2mT spatial variability is about 50% of that of LST in the area we studied; and (b) remote sensing data at 1 km is insufficient to accurately map the spatial variability of 2mT at the neighborhood scale. Therefore, satellite data is not used in the following to evaluate the model.

Unlike 2mT and LST, which show cooler temperatures at mountain tops in daytime and clear dependence on elevation, O_3 distribution over land shows more spatially continuous distribution with high concentration in the valleys (Figures 6e and 6f). Spatially, the largest variation occurs in areas with a high contrast of anthropogenic emissions such as the coastal region where urban areas and ocean meet and the mountain slopes that connect urban areas with higher altitude forest conditions. With this in mind, we can see that around water bodies (such as the Salton Sea) and coastal urban areas, the high variation of O_3 somewhat corresponds to the high variation of LST and 2mT.

To analyze the spatial variability in time series, we combine two paired quadrats (e.g., 1A and 1B, 2A and 2B, and 3A and 3B) to compute 2mT and O_3 inter-neighborhood spatial variability and compared them, respectively, with STD computed from the two WRF-Chem grid boxes covering the corresponding two quadrats (Figure 7). Overall, the correlations are poor (statistically insignificant) in the time series of the observed and simulated variability (STD) in each quadrat pair for both O_3 and 2mT, which further suggests that model simulation at 4 km is insufficient to describe the spatial variability of temperature and O_3 at neighborhood scale.

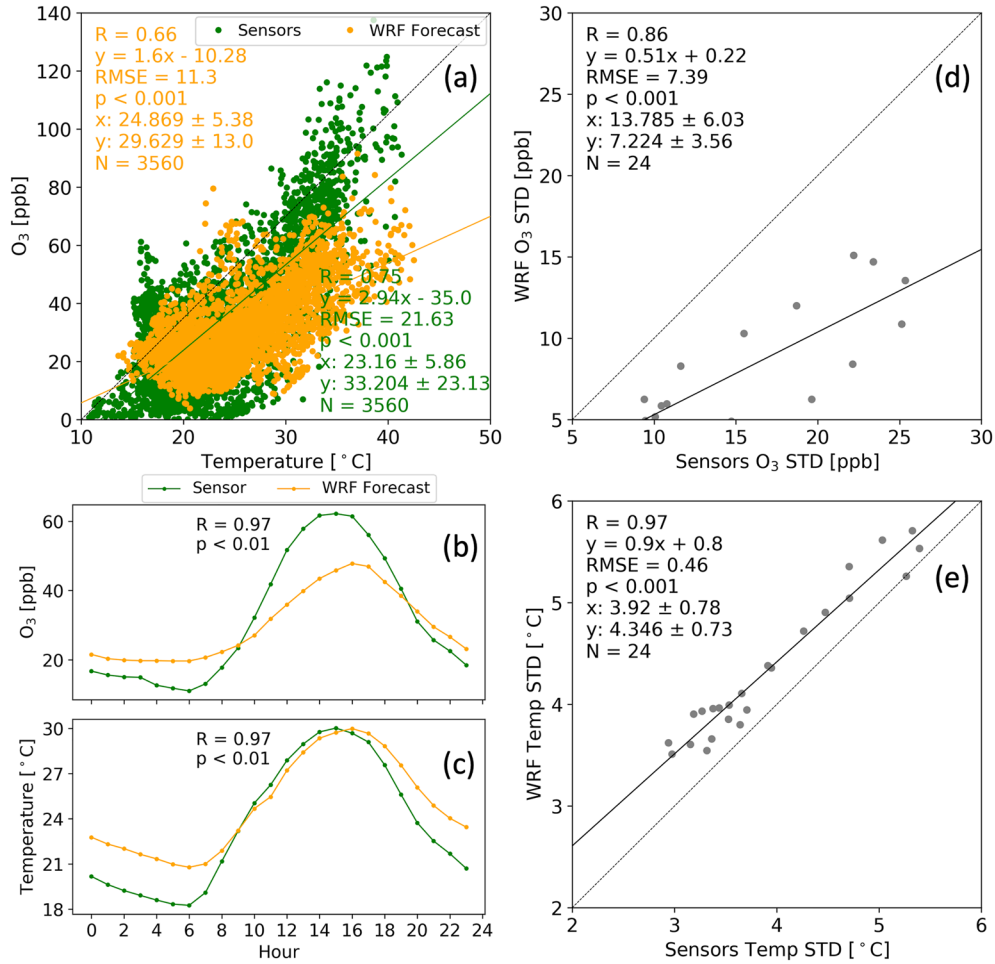

Figure 8. (a) Scatter plot of hourly temperature and O_3 observed (yellow dot) and predicted (green dot) at each quadrat. (b) Monthly mean hourly variation of O_3 from observations and predictions as a function of local hour. (c) Is the same as (b) but for temperature. (d) Scatter plot of the measured and modeled O_3 standard deviation at each hour. (e) Is the same as (d), but for temperature.

4.4. Relationships Between Variations of Temperature and O_3

Variation of 2mT and O_3 averaged over the six quadrats from both observations and WRF-Chem predictions was extensive (Figure 8). High correlation is found between the hourly variations of O_3 and 2mT, with R values of 0.66 and 0.75 in the observation and model predictions, respectively (Figure 8a). Modeled O_3 and 2mT peaked at 15:00 PDT and failed to reproduce the observed peak of O_3 and 2mT at 16:00 PDT (Figures 8b and 8c). However, the minima of O_3 and 2mT in the observations at ~6:00 PDT is well captured by the model (Figures 8b and 8c). Quantitatively, predictions show a low bias of O_3 and 2mT from 8:00 to 14:00 PDT of up to 20 ppb and 0.5°C, respectively, and the low bias continues for O_3 until 19:00 PDT. At nighttime from 20:00 PDT on the previous day to 8:00–9:00 PDT on the following day, model predictions overestimate both O_3 and 2mT by 5 ppb and 2–2.5°C, respectively (Figure 8b). Overall, modeled O_3 shows slightly better performance at nighttime, while modeled temperature shows slightly better performance in the daytime.

We also analyzed the degree that the model captures the temporal variation of O_3 and temperature for a given hour, respectively. The model slightly overpredicts the temporal variability for 2mT (Figure 8e) and largely underpredicts the temporal variability of O_3 by near a factor of two (Figure 8d), although in both cases the correlation is high and statistically significant. The contrast between Figures 7 and 8 suggests that overall, for both O_3 and 2mT, their temporal variability and covariability by hour is better captured in the model than their spatial variability (such as showed in Figure 7 and Figure S8 in Supporting Information S1).

This positive covaraition between O_3 and temperature is consistent with the findings in Nussbaumer and Cohen (2020) who used the multiple year of observation data and found that the O_3 formation in the Los Angeles basin overall is transiting from VOC-limited to NOx-limited regime, although the temperature and the weekly cycle of emission (with lower NOx in weekend) both play important roles. While reduction of both VOC and NOx emissions is needed to mitigate the occurrence of high O_3 events, the findings of this study suggest the importance of temperature as another key factor to be considered to resolve and predict neighborhood vulnerability. Not only because heat itself is harmful to public health, but also because it affects various chemical processes associated with O_3 formation (Pusede et al., 2015). Resolving the tree-O_3-VOC-temperature nexus is beyond the scope of this pilot study. But, overall, this study and others Nussbaumer and Cohen (2020) do suggest the conjecture that more trees appear to lead to decease of O_3 (especially during the hot summer days), likely due to the decrease of temperature by trees. Figure 8a clearly shows that a decrease of 1°C can lead to 1.6 ppb reduction in measured O_3 and 2.9 ppb in modeled O_3. More trees may lead to increase of VOC emissions, but in neighborhood settings, VOC emission from localized trees may dilute quickly in the atmosphere by the strong turbulent mixing in hot days. Detangling processes affect the impact of green space on O_3 formation also needs to consider that different tree types and sizes have different VOC potential (Gu et al., 2021) and response to temperature (Figure 3). Nevertheless, our community science project overall suggests that the green canopy potentially reduces O_3, and therefore, has the co-benefits to mitigate both air pollution and urban heat at the same time.

5. Summary and Discussions

We present the findings of a community science project that integrates community engagement, sensor data, satellite data, and model predictions to study how ozone pollution and temperature vary and covary, as well as the challenges in monitoring and predicting them at the neighborhood and intra-neighborhood scale. Several key findings are summarized as follows.

First, in urban settings, the spatial variations of land surface temperature, 2 m air temperature, and O_3 are substantial but are poorly resolved at the neighborhood and intra-neighborhood scale by MODIS at 1 km pixel resolution and WRF-Chem predictions at 4 km gridbox resolution. A model such as WRF-Chem can identify hotspots of variability at the regional scale and should be further improved at the local scale. The model can also predict well overall the variation of temperature from a community perspective. Second, in comparison to the performance of spatial variations, the diurnal variations of O_3 and 2 m air temperature and their covariation are relatively better resolved by the model. Both observations and models show moderate correlation between hourly O_3 and hourly temperature, but overall, models underestimate the covariation between temperature and O_3, in part because the model underpredicts the hourly fluctuations of O_3. Because the Los Angeles Basin is in the transitions between NO_x-limited and VOC-limited regime, exact cause for the underestimation of O_3 in here worthy further investigations. Prediction of temperature overall has much better performance than prediction of O_3 and requires much less spin-up than the minimum 12–36 hr required for ozone prediction. Models overpredict ozone at night and underpredict ozone at daytime, while predicted temperature generally has positive bias from late afternoon to the morning of the next day. Third, while our project had a relatively short duration (of 3 months), we show (with further support in the supplement) that the community science project has the unique potential to help (a) address science questions related to the spatial resolution needed to characterize the urban heat variaiblity (Figure S9 in Supporting Information S1) and, (b) quanitfy the potential value of ensemble forecasts by averaging the multiple forecasts made at different lead times to predict the spatial variability of temperature at the neighborhood scale (Figure S10 in Supporting Information S1).

This study is among the first attempts to use community science approach to study urban heat and ozone pollution at the intra- and inter-neighborhood scale. It underscored the previous studies that ozone in Los Angeles Basin overall is transitioning to the NO_x-limited and suggested that the green spacing can potentially serve as a sink for ozone. At high temperature conditions, for the O_3 formation, the impact of reduced temperature due to more trees may outweigh the impact of associated change of VOC from more trees, leading to an overall decrease of O_3. While more studies are needed, we found that the co-benefits to mitigate ozone pollution and high temperature at the same time via green spacing can be very revealing and appealing to the communities we engaged with. There are also a lot of enthusiasm among the community scientists for engaging with professional scientists. More community members are willing to engage with us to cope with environmental issues associated with their communities as they found, via this pilot project, that the science indeed work in most

cases, for example, toward predicting days with high ozone concentration and air temperature. Online, interactive, and real-time tools were also found to be critical for engaging community residents and helping them develop an interest in being community scientists. Together, community scientists and professional researchers can improve observations in various neighborhoods and help advance scientific studies that otherwise would not be possible to achieve. In turn, the scientific findings enabled by community scientists (such as the temperature variation with canopy type and size) can also amplify the scientific research to the neighborhood, thereby helping the community make objective and science-based decisions to mitigate urban heat and pollution at the same time.

Conflict of Interest

The authors declare no conflicts of interest relevant to this study.

Data Availability Statement

Satellite data can be obtained via https://ladsweb.modaps.eosdis.nasa.gov/archive/allData/6/MOD11A1/. The model data and community science data used in this paper can be obtained from https://doi.org/10.25820/data.006164. Details of the datasets can be found at Wang et al. (2022).

Acknowledgments
This work was supported by NASA Earth Science Citizen Science program (Grant #: NNX17AG61 A), NASA Health and Air Quality Applied Science Team (HAQST Grant #: 80NSSC21K0510), Earthwatch, and National Science Foundation (grant #:1924288). J. Wang also acknowledges the partial support from the University of Nebraska—Lincoln, the University of Iowa, and the USDA National Institute of Food and Agriculture (award number: 2019-67021-29227) for developing ESMC website. We would like to thank the community members and local partners who contributed their time and knowledge to the project.

References

Cabaraban, M. T., Kroll, C. N., Hirabayashi, S., & Nowak, D. J. (2013). Modeling of air pollutant removal by dry deposition to urban trees using a WRF/CMAQ/i-tree eco coupled system. *Environmental Pollution*, *176*, 123–133. https://doi.org/10.1016/j.envpol.2013.01.006

Chambers, L. H., McKeown, M. A., McCrea, S. A., Martin, A. M., Rogerson, T. M., & Bedka, K. M. (2017). CERES S'COOL project update: The evolution and value of a long-running education project with a foundation in NASA Earth science missions. *Bulletin of the American Meteorological Society*, *98*(3), 473–483. https://doi.org/10.1175/bams-d-15-00248.1

Churkina, G., Grote, R., Butler, T. M., & Lawrence, M. (2015). Natural selection? Picking the right trees for urban greening. *Environmental Science & Policy*, *47*, 12–17. https://doi.org/10.1016/j.envsci.2014.10.014

Elmore, K. L., Flamig, Z. L., Lakshmanan, V., Kaney, B. T., Farmer, V., Reeves, H. D., & Rothfusz, L. P. (2014). MPING: Crowd-sourcing weather reports for research. *Bulletin of the American Meteorological Society*, *95*(9), 1335–1342. https://doi.org/10.1175/bams-d-13-00014.1

Escobedo, F. J., & Nowak, D. J. (2009). Spatial heterogeneity and air pollution removal by an urban forest. *Landscape and Urban Planning*, *90*(3), 102–110. https://doi.org/10.1016/j.landurbplan.2008.10.021

Fast, J. D., Gustafson, W. I. Jr., Easter, R. C., Zaveri, R. A., Barnard, J. C., Chapman, E. G., et al. (2006). Evolution of ozone, particulates, and aerosol direct radiative forcing in the vicinity of Houston using a fully coupled meteorology-chemistry-aerosol model. *Journal of Geophysical Research*, *111*, D21305. https://doi.org/10.1029/2005jd006721

Ge, C., Wang, J., & Reid, J. S. (2014). Mesoscale modeling of smoke transport over the southeast Asian maritime continent: Coupling of smoke direct radiative effect below and above the low-level clouds. *Atmospheric Chemistry and Physics*, *14*(1), 159–174. https://doi.org/10.5194/acp-14-159-2014

Ge, C., Wang, J., Reid, J. S., Posselt, D. J., Xian, P., & Hyer, E. (2017). Mesoscale modeling of smoke transport from equatorial southeast Asian Maritime Continent to the Philippines: First comparison of ensemble analysis with in situ observations. *Journal of Geophysical Research: Atmospheres*, *122*(10), 5380–5398. https://doi.org/10.1002/2016JD026241

Grell, G., Peckham, S. E., Schmitz, R., McKeen, S. A., Frost, G., Skamarock, W. C., & Eder, B. (2005). Fully coupled "online" chemistry within WRF model. *Atmosperhic Environment*, *39*, 6957–6975. https://doi.org/10.1016/j.atmosenv.2005.04.027

Griffin, D., Zhao, X., McLinden, C. A., Boersma, F., Bourassa, A., Dammers, E., et al. (2019). High-resolution mapping of nitrogen dioxide with TROPOMI: First results and validation over the Canadian oil sands. *Geophysical Research Letters*, *46*(2), 1049–1060. https://doi.org/10.1029/2018gl081095

Gu, S., Guenther, A., & Faiola, C. (2021). Effects of anthropogenic and biogenic volatile organic compounds on Los Angeles air quality. *Environmental Science & Technology*, *55*(18), 12191–12201. https://doi.org/10.1021/acs.est.1c01481

Harlan, S. L., Declet-Barreto, J. H., Stefanov, W. L., & Petitti, D. B. (2013). Neighborhood effects on heat deaths: Social and environmental predictors of vulnerability in maricopa county, Arizona. *Environmental Health Perspectives*, *121*(2), 197–204. https://doi.org/10.1289/ehp.1104625

Hong, C., Zhang, Q., Zhang, Y., Davis, S. J., Tong, D., Zheng, Y., et al. (2019). Impacts of climate change on future air quality and human health in China. In *Proceedings of the national academy of sciences* (Vol. 116(35), pp. 17193–17200). https://doi.org/10.1073/pnas.1812881116

IPCC. (2021). *Climate change 2021: The physical science basis. Contribution of working group I to the sixth assessment report of the intergovernmental panel on climate change [Masson-Delmotte*. In V. P. Zhai, A. Pirani, S. L. Connors, C. Péan, S. Berger, N. Caud et al. (Eds.), Cambridge University Press. In Press.

Jacob, D. J., & Winner, D. A. (2009). Effect of climate change on air quality. *Atmospheric Environment*, *43*(1), 51–63. https://doi.org/10.1016/j.atmosenv.2008.09.051

Kennedy, T. J., & Henderson, S. (2003). The GLOBE program: Bringing together students, teachers and scientists to increase scientific understanding of the Earth through research. *Children, Youth, and Environments*, *13*(2), 217–227. https://doi.org/10.1007/978-94-017-3368-7_15

Mahajan, S., Kumar, P., Pinto, J. A., Riccetti, A., Schaaf, K., Camprodon, G., et al. (2020). A citizen science approach for enhancing public understanding of air pollution. *Sustainable Cities and Society*, *52*, 101800. https://doi.org/10.1016/j.scs.2019.101800

Morani, A., Nowak, D. J., Hirabayashi, S., & Calfapietra, C. (2011). How to select the best tree planting locations to enhance air pollution removal in the MillionTreesNYC initiative. *Environmental Pollution*, *159*(5), 1040–1047. https://doi.org/10.1016/j.envpol.2010.11.022

National Academies of Sciences, E. (2018). *Learning through citizen science: Enhancing opportunities by design*. The National Academies Press & Medicine.

Nolte, C. G., Spero, T. L., Bowden, J. H., Mallard, M. S., & Dolwick, P. D. (2018). The potential effects of climate change on air quality across the conterminous U.S. at 2030 under three Representative Concentration Pathways. *Atmospheric Chemistry and Physics*, *18*(20), 15471–15489. https://doi.org/10.5194/acp-18-15471-2018

Nowak, D. J., Hirabayashi, S., Bodine, A., & Greenfield, E. (2014). Tree and forest effects on air quality and human health in the United States. *Environmental Pollution*, *193*, 119–129. https://doi.org/10.1016/j.envpol.2014.05.028

Nussbaumer, C. M., & Cohen, R. C. (2020). The role of temperature and NOx in ozone trends in the Los Angeles Basin. *Environmental Science & Technology*, *54*(24), 15652–15659. https://doi.org/10.1021/acs.est.0c04910

Pataki, D. E., Carreiro, M. M., Cherrier, J., Grulke, N. E., Jennings, V., Pincetl, S., et al. (2011). Coupling biogeochemical cycles in urban environments: Ecosystem services, green solutions, and misconceptions. *Frontiers in Ecology and the Environment*, *9*(1), 27–36. https://doi.org/10.1890/090220

Pusede, S. E., Steiner, A. L., & Cohen, R. C. (2015). Temperature and recent trends in the chemistry of continental surface ozone. *Chemical Reviews*, *115*(10), 3898–3918. https://doi.org/10.1021/cr5006815

Racherla, P. N., & Adams, P. J. (2008). The response of surface ozone to climate change over the Eastern United States. *Atmospheric Chemistry and Physics*, *8*(4), 871–885. https://doi.org/10.5194/acp-8-871-2008

Samad, A., & Vogt, U. (2020). Investigation of urban air quality by performing mobile measurements using a bicycle (MOBAIR). *Urban Climate*, *33*, 100650. https://doi.org/10.1016/j.uclim.2020.100650

Sha, T., Ma, X., Zhang, H., Janechek, N., Wang, Y., Wang, Y., et al. (2021). Impacts of soil NOx emission on O_3 air quality in rural California. *Environmental Science & Technology*, *55*(10), 7113–7122. https://doi.org/10.1021/acs.est.0c06834

Shiflett, S. A., Liang, L. L., Crum, S. M., Feyisa, G. L., Wang, J., & Jenerette, G. D. (2017). Variation in the urban vegetation, surface temperature, air temperature nexus. *The Science of the Total Environment*, *579*, 495–505. https://doi.org/10.1016/j.scitotenv.2016.11.069

Shirk, J. L., Ballard, H. L., Wilderman, C. C., Phillips, T., Wiggins, A., Jordan, R., et al. (2012). Public participation in scientific research: A framework for deliberate design. *Ecology and Society*, *17*(2). https://doi.org/10.5751/es-04705-170229

Tomlinson, C. J., Chapman, L., Thornes, J. E., & Baker, C. (2011). Remote sensing land surface temperature for meteorology and climatology: A review. *Meteorological Applications*, *18*(3), 296–306. https://doi.org/10.1002/met.287

Tong, Z., Whitlow, T. H., MacRae, P. F., Landers, A. J., & Harada, Y. (2015). Quantifying the effect of vegetation on near-road air quality using brief campaigns. *Environmental Pollution*, *201*, 141–149. https://doi.org/10.1016/j.envpol.2015.02.026

Wan, Z., Zhang, Y., Zhang, Q., & Li, Z. L. (2004). Quality assessment and validation of the MODIS global land surface temperature. *International Journal of Remote Sensing*, *25*(1), 261–274. https://doi.org/10.1080/0143116031000116417

Wang, J., Castro-Garciaa, L., Jenerettec, G. D., Chandlerd, M., Ge, C., Kucera, D., et al. (2022). *Forecast and citizen observations for temperature and ozone for Los Angeles area*. https://doi.org/10.25820/data.006164

Wang, J., Ge, C., Yang, Z., Hyer, E. J., Reid, J. S., Chew, B.-N., et al. (2013). Mesoscale modeling of smoke transport over the southeast Asian Maritime Continent: Interplay of sea breeze, trade wind, typhoon, and topography. *Atmospheric Research*, *122*, 486–503. https://doi.org/10.1016/j.atmosres.2012.05.009

Zhang, H., Wang, J., García, L. C., Ge, C., Plessel, T., Szykman, J., et al. (2020). Improving surface PM2.5 forecasts in the U.S. using an ensemble of chemical transport model outputs, part I: Bias correction with surface observations in non-rural areas. *Journal of Geophysical Research: Atmospheres*, e2019JD032293.